

# AERODYNAMIC ANALYSIS OF MULTI-WINGLETS FOR LOW SPEED AIRCRAFT

**Cosin, R. , Catalano, F.M. , Correa, L.G.N. , Entz, R.M.U.**  
**Engineering School of São Carlos - University of São Paulo**

**Keywords:** *multi-winglets, induced drag, tip sails, aerodynamic efficiency*

## Abstract

*An analysis of multi-winglets as a device for reducing induced drag in low speed aircraft is carried out, based on experimental investigations of a wing-body half model at  $Re = 4 \cdot 10^5$ .*

*A baseline and six other different multi-winglets configurations were tested. The device led to 32% improvement in the Oswald efficiency factor, representing an increase of 7% in the maximum aerodynamic efficiency. Improvements of 12% in the maximum rate of climb and 7% in the maximum range were also obtained.*

*The pressure distribution was measured to verify global and local effects of the multi-winglets, showing only a small influence of the device on the wing loading. Structural investigations were also carried out, as well as wake surveys using a seven hole Pitot probe that indicated significant changes in the flow field near the wingtip.*

## 1 Introduction

Induced drag is caused by the wingtip vortex, an unavoidable collateral effect of lift generation in a finite wing. It has been proven that modifications in the wingtip or the use of wingtip devices can minimize the induced drag expressively. Extensive research was conducted with the objective of studying these devices, as well as proposing new designs and approaches.

In this context, the present work investigates the potential use of multi-winglets to decrease the induced drag in a light aircraft, enhancing the

aerodynamic efficiency and the performance.

Modifications in the wingtip can either move the vortices away in relation to the aircraft longitudinal axis or reduce their intensity [1]. Some of these devices such as winglets [2], tip-sails [3, 4, 5] and multi-winglets [6] take energy from the spiraling airflow in this region to create additional traction. This makes possible to achieve expressive gains on efficiency. Whitcomb [2], for example, shows that winglets could increase wing efficiency in 9% and decrease the induced drag in 20%. Some devices also break up the vortices into several parts, each one with less intensity. This facilitates their dispersion, an important factor to decrease the time interval between takeoff and landings at large airports [7].

A comparison of the wingtip devices [1] shows that winglets have higher aerodynamic benefits up to Mach 1.0, but may create structural problems due to the bending moment increase at the wing root. Tip-sails have the same drag reduction at low lift conditions, with a lower bending moment at the wing root.

In general aviation, research on wingtip devices was carried out for sailplanes, even though their wings have a large aspect ratio. Smith and Komerath [6] mention the development work of winglets for sailplanes, with wind tunnel testing of scale models. Another important application is the use in agricultural airplanes, as the wingtip vortex is an important factor in the dispersion of pulverized fluid. In this field an important work is that of Coimbra [8], which compares several wingtip devices and analyzes the effects on pulverization.

## 2 Experimental set-up

The tests were carried out in the LAE 2, a closed circuit low speed wind tunnel with turbulence level of 0.25% at 30m/s. The test section is 1.7m wide, 1.3m high and it has 3.6m of length [9].

All the experiments were done at  $Re = 4.0 \cdot 10^5$ , except the wake measurements, which were conducted at  $Re = 3.1 \cdot 10^5$ . This corresponds to freestream velocities of 30.0m/s and 23.4m/s, respectively.

### 2.1 General model characteristics

A half model was designed and built based on a single engine trainer aircraft. This airplane has a high wing configuration and is under development at the Engineering School of São Carlos.

The model consists of a 1 : 6 scale wing-body configuration, and its full span aspect ratio is 8. It has a rectangular wing with a dihedral angle of  $1.50^\circ$  and washout of  $1.25^\circ$ . A NACA 23015 airfoil is used on the entire span.

The fuselage was designed to accommodate all the pressure scanner modules and the installation accessories. The wing support allows adjusting of the dihedral and the wing incidence. In the model, the wing chord is 216.5mm. Landing gear and empennage were omitted.

A very smooth surface finish was built in order to avoid unintentional forced transition. On the upper and lower surface there are 248 pressure measuring orifices in 8 wing sections, with higher density of pressure taps at the leading edge and wingtip. The model also has a 30mm stand-off to minimize the effects of the tunnel boundary layer.

### 2.2 Variable configurations multi-winglets

The wingtip device is a variable configuration multi-winglets with three tip sails. Those are attached to a movable mechanism that allows the adjustment of the cant angle and incidence for each sail independently. In order to avoid undesirable configuration change during experiments, a locking mechanism was built. All pieces of the wingtip device were manufactured in polyamide



Fig. 1 Model prepared for the wing tunnel testing

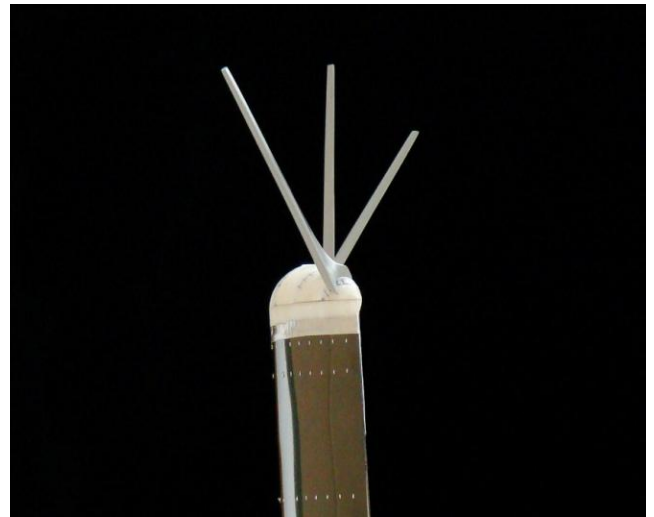


Fig. 2 Multi-winglets details

using SLS "selective laser sinterization", a fast prototyping process.

The sails are non swept at the quarter-chord, their taper ratio is 0.45 and the aspect ratios are 2.7, 3.1 and 3.5. Profiles, twist distribution and other geometric parameters were defined in order to produce a desirable incidence angle for the winglets, considering the highly spiraling flow induced by the wingtip vortex, resulting in high cambered airfoils in the sails roots and symmetrical in the tips. The initial estimation of the flow field was performed with CFD calculations.

Six configurations are compared with the baseline (no sails configuration). The cant angles combinations are listed in Tab. 1 and they

Config.	Cant angle		
	Winglet 1	Winglet 2	Winglet 3
1	-30	0	30
2	45	15	-15
3	-15	-30	-45
4	60	30	0
5	45	30	15
6	30	15	0

**Table 1** Cant angles

are based on the best results available in [10].

Trips for forcing transition were not used during most of the tests, as the objective of the present work is the study of the lift dependent drag. One case with forced transition was evaluated and compared to the untripped wing case. The fully turbulent case had slight lower lift coefficients, however, no changes in the stall characteristics due to the forced transition were detected.

### 2.3 Instruments and measures

Drag and lift were measured with the incidence angle varying from  $4^\circ$  to  $+20^\circ$  with a strain gage balance. The accuracy is 0.7% of the maximum loading, representing  $\pm 1.0N$  and  $\pm 0.19N$  for lift and drag, respectively, and the incidence angle was measured with an accuracy of  $\pm 0.1^\circ$ . Pressure measurements were carried out using Scani-valves ZOC 33/64PxX2 with a  $\pm 2.5psid$  transducer that provides  $\pm 0.10\%$  FS accuracy.

A strain gage was installed on the wing spar, which is assumed to withstand all the aerodynamic loads. It was calibrated to measure the bending moment on the wing root, which is useful to verify the influence of the device on structural loading. Measurements of the velocity field at the wingtip wake were also carried out using a seven hole Pitot probe with piezoresistive pressure transducers.

## 3 Results and discussion

### 3.1 Wind tunnel corrections

Wind tunnel wall corrections and stand-off geometry were computed with CFD simulations of the baseline configuration and the results were compared with the respective experimental data.

The CFD computations were performed with ANSYS CFX, using the shear stress transport turbulence model (SST) and the  $\gamma - \theta$  transition model. Mesh generation was done with ANSYS ICEM CFD, using unstructured grids based on the real model, which geometry was confirmed with a high precision three-dimensional measuring arm.

CATIA V5 was used to generate the geometry from the model surface scan data. Mesh convergence and validation studies were performed using the wind tunnel boundary conditions in the simulations. Once validated, the numerical model was evaluated for the wind tunnel conditions, considering the walls. This model was also used to compute the flow parameters for a condition with open boundaries.

The results of both simulations were compared, giving relations of the aerodynamic coefficients in the wind tunnel and in flight conditions, which were then applied to define corrections for typical analytical relations.

### 3.2 Aerodynamic characteristics

#### 3.2.1 Lift and drag influence

Data obtained with the measured aerodynamic forces shows a significant increase in the lift curve slope when compared with the basic wing, achieving higher lift coefficients for most angles of attack, as in Fig. 3. This can be explained mainly by the wing loading increase near the tip, as in Fig. 8 and Fig. 9, in addition to the lift of the each winglet itself, even with their small area. The lift curve slope was increased from 4.8 to 5.3 in configuration 5, which represents 11%.

An improvement on the maximum lift coefficient is also observed for the six studied configurations in Fig. 3. The stall angle of attack is near the same for the basic wing and all configurations. The maximum lift increase can be as-

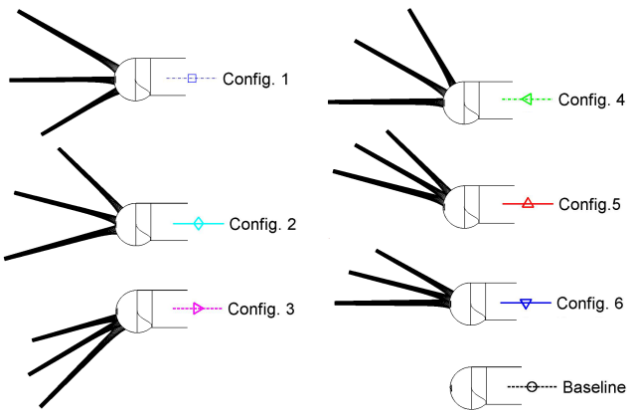
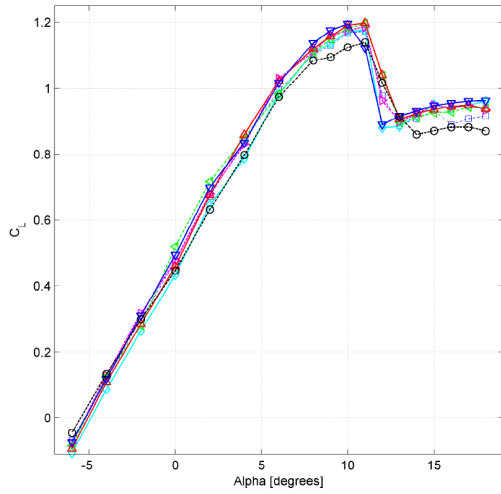


**Fig. 3** Lift coefficient and the studied configurations

sociated with a lower pressure on the tip region near the trailing edge on the upper surface. The maximum lift coefficient raised from 1.14 to 1.20 in configuration 6.

The effects of the multi-winglets on drag at most of angles of attack are of small magnitude. It can be seen that for angles of attack up to  $2^\circ$ , the device produces a slightly more drag than the basic wing. For higher angles, as in Fig. 4, the reductions of the induced drag become more expressive and the total drag is reduced until the stall. These characteristics are consequence of the additional zero lift drag caused by the sails and the induced drag reduction, which is the prominent in most conditions.

The drag polar in Fig. 5 shows that the efficiency increase is due to greater lift and slightly lower drag, as the multi-winglets create a scattered vortex system, besides weaker and further

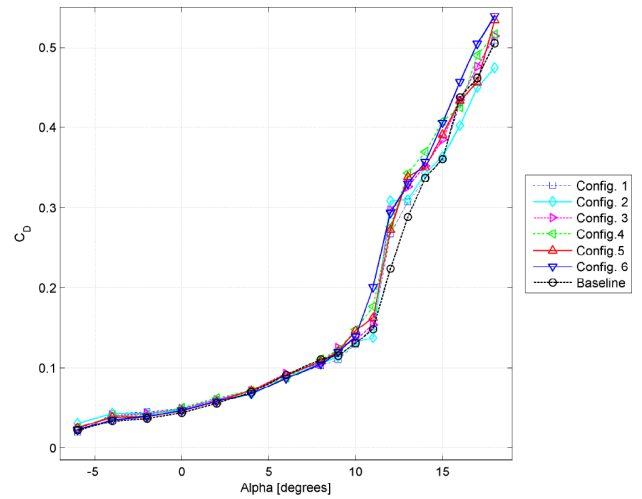


**Fig. 4** Drag coefficient

from the wing tip, with lower influence over the wing. The induced drag reduction is better understood in Fig. 6, which shows that configurations with multi-winglets have a lower slope in the total drag as a function of  $C_L^2$ .

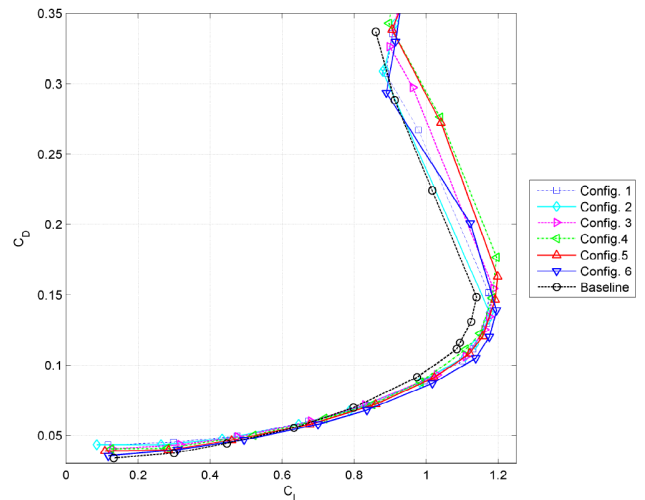


**Fig. 5** Drag polars

The lift slope, zero lift drag and Oswald efficiency factor were computed at the linear interval of the  $C_L \times \alpha$  curve and their values are in Table 2. The reductions on the lift dependent drag are confirmed by the significant increases of up to 32% in the Oswald efficiency factor. Despite the clear induced drag reduction, there is an undesirable increase in the zero lift drag. Roughly, wings with the device are more efficient only for lift co-

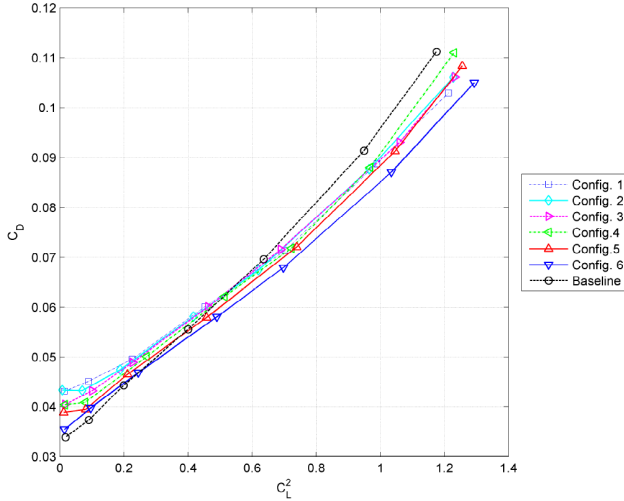


Fig. 6 Induced drag

Config.	$C_{L\alpha}$	$e$	$C_{D_0}$	$L/D$
1	5.081	0.855	0.040	11.74
2	5.131	0.846	0.040	11.67
3	5.117	0.787	0.038	11.59
4	5.078	0.796	0.037	11.83
5	5.335	0.781	0.036	11.93
6	5.141	0.801	0.035	12.29
Baseline	4.822	0.648	0.032	11.45

Table 2 Experimental coefficients for several configurations

efficients greater than  $0.45 \pm 0.05$ . This negative effect is clearly overestimated in the wind tunnel tests due to the sails chord Reynolds number, in which the maximum value is as low as  $Re = 0.7 \cdot 10^4$ , what bring undesirable effects that are not expected in full scale implementations.

### 3.2.2 Pressure data

Pressure distributions from the wind tunnel tests show that changes in the wing loading are very small for most configurations, as in Fig. 8 and Fig. 9. However, there is some increase in the loading at the tip region, as expected due to the higher lift coefficient.

The baseline configuration has a high pressure region at the wingtip near the trailing edge. The multi-winglets were able to reduce the pressure at that region due to the vorticity reduction, indicating a decrease of the wingtip vortex influence.

Pressure data for  $\alpha = 13^\circ$  also shows that the multi-winglets do not change the main stall characteristics. In spite of small variations in the stall angle of attack of around  $1.0^\circ$ , the separated region is almost the same for the basic wing and for the other configurations.

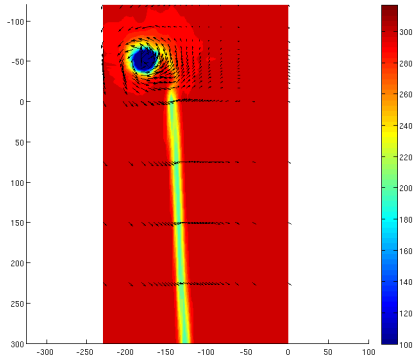
### 3.2.3 Wake analysis

The three-dimensional velocity components in the wake were mapped for  $\alpha = 4^\circ$  in the basic wing and three other configurations. The velocity contour shows a very expressive change in the tip vortex when compared to the baseline configuration, as in Fig. 7. As expected, the winglets reduce the main wingtip vortex intensity and create weaker vortices at the sails tips, which are strongly dependent on the configuration parameters. It is also possible to notice a region with a wider wake region near the sails roots, what indicates higher friction drag, possibly caused by typical low Reynolds number effects such as laminar separation bubbles.

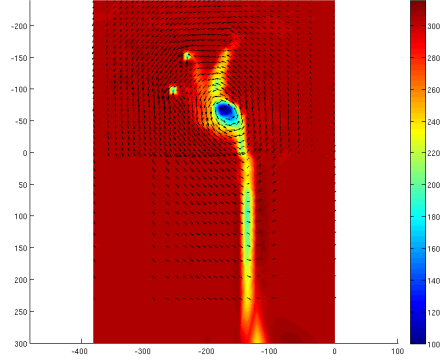
### 3.2.4 Flow visualization

Steady flow visualization for configuration 6 is in Fig. 10. Some clear interferences between the winglets tip vortex and the downstream sails are visible, as well as the interference of the wingtip on the sails near their roots. Laminar separation bubbles (indicated by the white regions) are present over more than a quarter of the chord of the upper surface in all winglets.

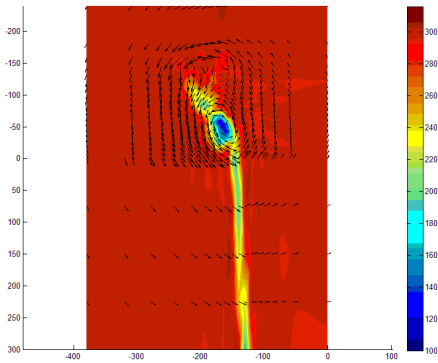
This is a result of paramount importance for the analysis of this work, as they confirm the hypothesis made on the previous sections and indicate that parasite drag values will be considerably higher than that of a real implementation.



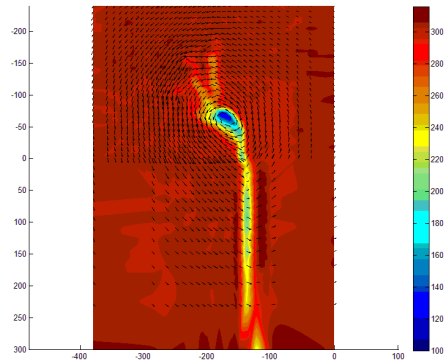
(a) Baseline



(b) Configuration 1



(c) Configuration 3



(d) Configuration 6

**Fig. 7** Wake survey

# AERODYNAMIC ANALYSIS OF MULTI-WINGLETS FOR LOW SPEED AIRCRAFT

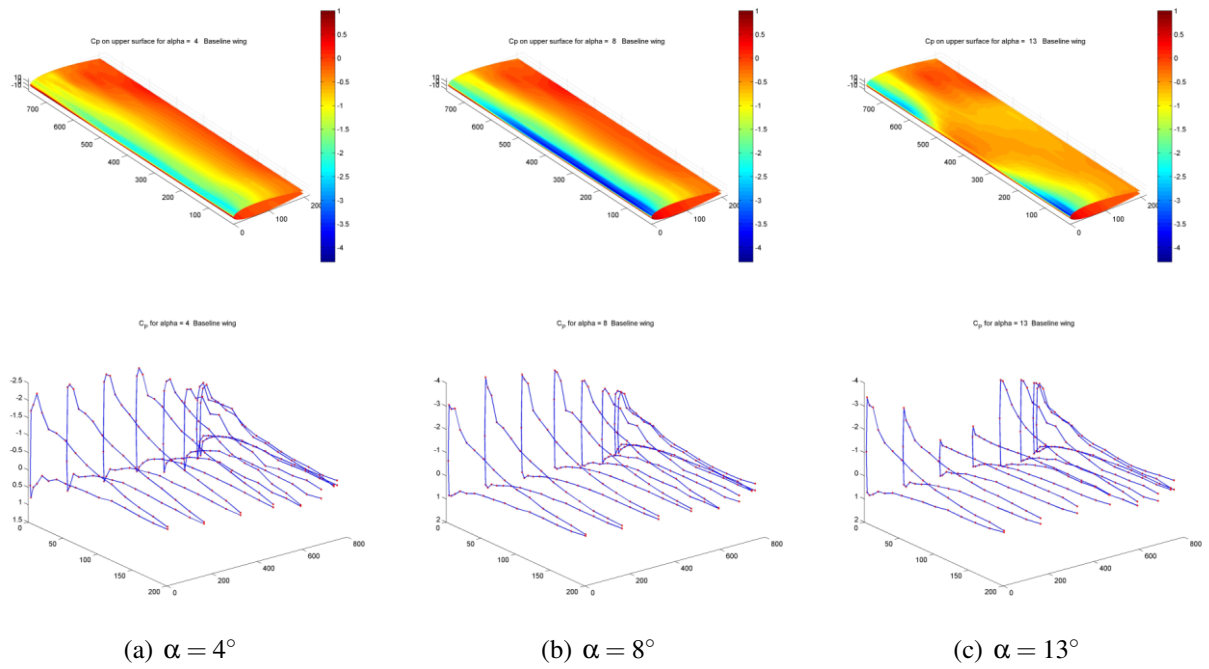


**Fig. 8** Pressure coefficient for the baseline configuration

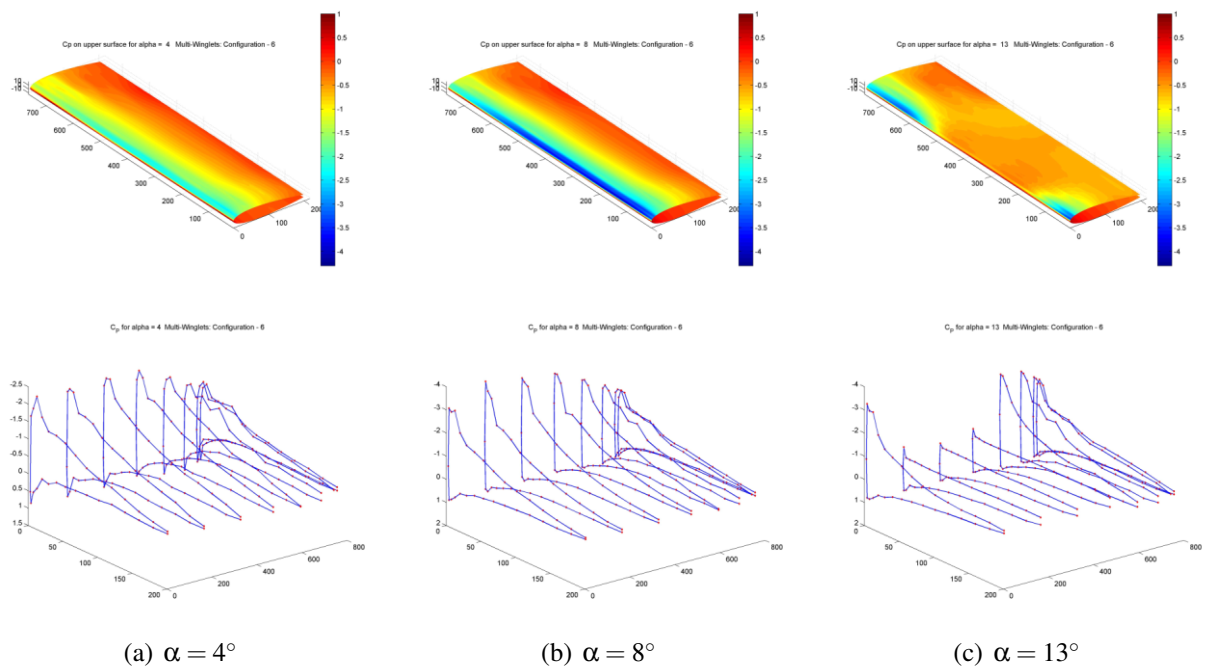


**Fig. 9** Pressure coefficient for configuration 6

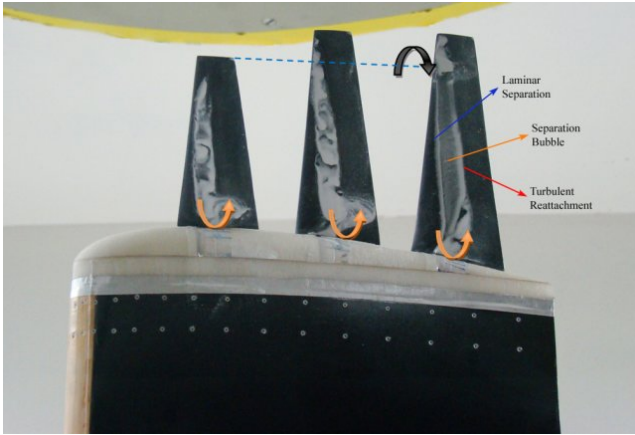


Fig. 10 Surface flow visualization

### 3.3 Performance analysis

#### 3.3.1 Aerodynamic efficiency

During the experimental investigation, significant changes of the lift-drag ratio were found with the use of these devices, as in Fig. 11. These improvements are observed especially at high angles of attack, in which the induced drag represents a significant fraction of the total drag.

L/D improvements were around 11% for  $\alpha = 8^\circ$  in configuration 6. The maximum efficiency was improved by up to 7.3% and for all the cases it occurs at  $\alpha = 4^\circ$ . For higher angles of attack, all the tested configurations had benefits in the lift to drag ratio, although efficiency enhancements were observed since  $\alpha = 0$ . As consequence of the increased efficiency, improvements in all performance parameters are expected and it was confirmed by the analysis of the rate of climb and range.

#### 3.3.2 Performance analysis

Reductions of induced drag with the use of multi-winglets led to an expressive increase in the maximum rate of climb, as it is proportional to the parameter  $C_L^{1.5}/C_D$ . Fig. 12 shows up to 14% of improvement in this parameter for configuration 6. There is also there an increase of 12% in the maximum rate of climb for this configuration, represented by the highest value of  $C_L^{1.5}/C_D$ . All other configurations have improvements of at least 12% in this parameter for angles of attack greater than  $4^\circ$ .

For propeller driven aircrafts, the range influence of the multi-winglets is directly related to the lift to

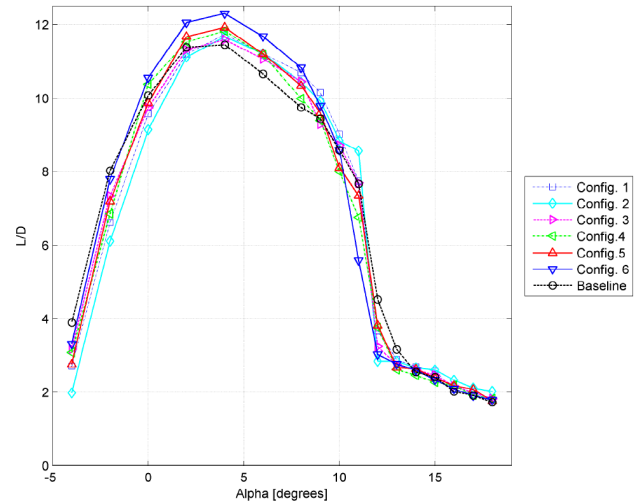


Fig. 11 Aerodynamic efficiency

$\alpha$	L/D change (%)					
	C. 1	C. 2	C. 3	C. 4	C. 5	C. 6
-2	-23.9	-8.5	-17.6	-14.6	-10.3	-2.9
0	-9.4	-3.4	-5.0	3.1	-2.0	4.7
2	-2.4	-0.6	-1.7	1.3	2.6	5.9
4	1.9	1.2	2.5	3.3	4.1	7.3
6	5.2	3.8	5.2	4.9	5.1	9.6
8	7.1	7.3	9.7	2.5	6.1	11.1
9	5.1	-1.6	7.6	-0.5	1.7	3.7
10	3.0	1.5	5.0	-6.9	-5.6	0.0
11	11.7	0.3	1.0	-11.9	-4.2	-27.2

Table 3 Experimental coefficients for several configurations

drag ratio, considering a condition with constant lift coefficient. All studied configurations then lead to potential improvements in range for most practical cruise lift coefficients. The maximum range, related to the maximum efficiency condition, is increased of 7.3% for the best configuration and at least 1.2% for the other configurations. During cruise at low lift coefficient, the raise in zero lift drag compensates the induced drag reductions, making the benefits of the device negligible. However, for higher angles of attack, especially  $8^\circ$ , up to 11% of increase in range are expected.

#### 3.3.3 Structural loading analysis

Direct measurement of the bending moment was obtained with the strain gage on the wing spar. The results revealed that the multi-winglets do not signifi-

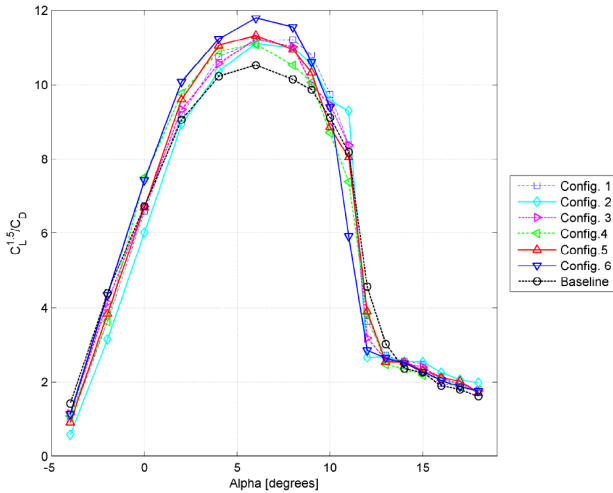


Fig. 12 Rate of climb factor

cantly increase the structural loading, as the relation between lift and bending moment is nearly the same for the baseline and other configurations (cf. Fig. 13), with the exception of configuration 1.

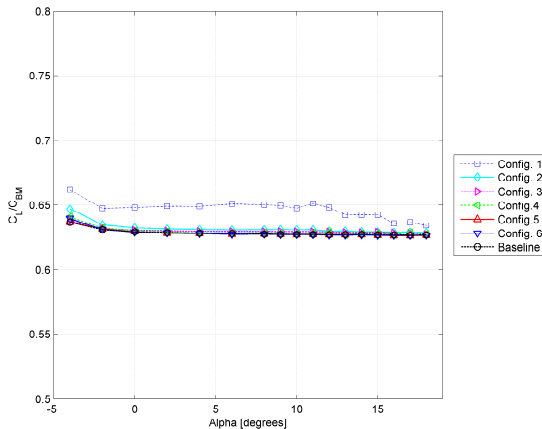


Fig. 13 Lift coefficient over non-dimensional bending moment

#### 4 Conclusion

Potential improvements with the use of multi-winglets were shown with experimental data. This wingtip device led to significant increase in the performance parameters, with a 7.3% gain in the maximum aerodynamic efficiency and improvements of up to 11% for other conditions. The maximum estimated rate of climb factor was also increased by 12%.

Aerodynamic characteristics of the multi-winglets revealed improvements in the lift slope as well as expressive reduction of induced drag, represented by a 32% increase in the Oswald efficiency factor. However, additional parasite drag offsets those benefits at low lift conditions.

The aerodynamic loading was slightly increased near the wingtip, but general aspects of the baseline wing were maintained, the most important being stall characteristics. Structural loading due to lift was not significantly changed with the use of the winglets, bringing no negative structural effects.

In a nutshell, results show that multi-winglets can be a promising approach for controlling wingtip vortices. From this work, however, it is evident that research on higher Reynolds number is still needed to establish realistic break even boundaries for the use of this technology. However, the results presented show that this is a promising approach as a wingtip device.

It is possible to see in Fig. 5 that there is an increase in  $C_D$  for low  $C_L$  conditions. This is mainly due to separation regions at the winglets root, as the local flow incidence angle is highly negative at low  $C_L$ . This phenomena also happens with single winglets, as the drag due to the root separation is larger than the thrust generated by the winglet at low  $C_L$ . These separations are more critical at low Reynolds number, such as in the wind tunnel of the present work.

#### Acknowledgements

The authors would like to thank the State of São Paulo Research Foundation - FAPESP for sponsoring this project and the Engineering School of São Carlos for financing the presentation of this work.

#### References

- [1] S. A. Kravchenko, “The application of the wingtip lifting surfaces for practical aerodynamic,” in *ICAS*, 1338-1349, 1996.
- [2] R. T. Whitcomb, “A design approach and selected wind-tunnel results at high subsonic speeds for wing-tip mounted winglets,” tech. rep., NASA TN-D-8260, 1976.
- [3] J. J. Spillman, “The use of wing tip sails to reduce vortex drag,” *Aeronautical Journal*, vol. 82, pp. 387–395, 1978.
- [4] J. J. Spillman and M. McVitie, “Wing tip sails which give lower drag at all normal flight

- speeds,” *Aeronautical Journal*, vol. 88, pp. 362–369, 1984.
- [5] J. J. Spillman, “Wing tip sails; progress to date and future developments. aeronautical journal, vol 91 no 9xx, pp 445-543, 1987.,” *Aeronautical Journal*, vol. 91, pp. 445–543, 1987.
- [6] M. J. Smith, N. Komerath, R. Ames, O. Wong, and J. Pearson, “Performance analysis of a wing with multiple winglets,” in *AIAA Applied Aerodynamics, AIAA 2001-2407*, 2001.
- [7] U. La Roche and S. Palffy, “Wing-grid, a novel device for reduction of induced drag on wings,” in *ICAS*, 1996.
- [8] R. Coimbra and F. Catalano, “Estudo experimental sobre pontas de asa para uma aeronave agrícola,” *Revista Brasileira de Engenharia Agrícola e Ambiental*, vol. 3, pp. 99–105, 1999.
- [9] F. Catalano, “The new closed circuit wind tunnel of the aircraft laboratory of university of são paulo,” in *16th Brazilian Congress of Mechanical Engineering*, 2001.
- [10] H. D. C. Munoz and F. Catalano, “Experimental analysis of the aerodynamic characteristics adaptive of multi-winglets,” *J Aerospace Eng*, vol. 220, pp. 209–216, 2004.

### Copyright Statement

The authors confirm that they, and/or their company or organization, hold copyright on all of the original material included in this paper. The authors also confirm that they have obtained permission, from the copyright holder of any third party material included in this paper, to publish it as part of their paper. The authors confirm that they give permission, or have obtained permission from the copyright holder of this paper, for the publication and distribution of this paper as part of the ICAS2010 proceedings or as individual off-prints from the proceedings.